AMERICAN ACADEMY OF OPHTHALMOLOGY®

Digital Gonioscopy Based on Three-dimensional Anterior-Segment OCT

An International Multicenter Study

Fei Li, MD, PhD,[1,] Yifan Yang, MSc,[2,*] Xu Sun, PhD,[3,*] Zhen Qiu, MSc,[2] Shihao Zhang, MSc,[2] Tin Aung Tun, MBBS,[4,5] Baskaran Mani, DNB,[4,5] Monisha Esther Nongpiur, MD, PhD,[4,5] Sunee Chansangpetch, MD, BPH,[6] Kitiya Ratanawongphaibul, MD,[6] Anita Manassakorn, MD,[6] Visanee Tantisevi, MD,[6] Prin Rojanapongpun, MD,[6] Fengbin Lin, MD,[1] Weijing Cheng, MD,[1] Rouxi Zhou, MD, PhD,[1] Yuhong Liu, BSMed,[1] Yu Chen, BSMed,[1] Jian Xiong, MD, PhD,[1] Mingkui Tan, PhD,[2] Tin Aung, MD, PhD,[4,5,7] Yanwu Xu, PhD,[3,4] Daniel S.W. Ting, MD, PhD,[4,5] Xiulan Zhang, MD, PhD[1]*

Purpose: To develop and evaluate the performance of a 3-dimensional (3D) deep-learning–based automated digital gonioscopy system (DGS) in detecting 2 major characteristics in eyes with suspected primary angle-closure glaucoma (PACG): (1) narrow iridocorneal angles (static gonioscopy, Task I) and (2) peripheral anterior synechiae (PAS) (dynamic gonioscopy, Task II) on OCT scans.

Design: International, cross-sectional, multicenter study.

Participants: A total of 1.112 million images of 8694 volume scans (2294 patients) from 3 centers were included in this study (Task I, training/internal validation/external testing: 4515, 1101, and 2222 volume scans, respectively; Task II, training/internal validation/external testing: 378, 376, and 102 volume scans, respectively).

Methods: For Task I, a narrow angle was defined as an eye in which the posterior pigmented trabecular meshwork was not visible in more than 180° without indentation in the primary position captured in the dark room from the scans. For Task II, PAS was defined as the adhesion of the iris to the trabecular meshwork. The diagnostic performance of the 3D DGS was evaluated in both tasks with gonioscopic records as reference.

Main Outcome Measures: The area under the curve (AUC), sensitivity, and specificity of the 3D DGS were calculated.

Results: In Task I, 29.4% of patients had a narrow angle. The AUC, sensitivity, and specificity of 3D DGS on the external testing datasets were 0.943 (0.933–0.953), 0.867 (0.838–0.895), and 0.878 (0.859–0.896), respectively. For Task II, 13.8% of patients had PAS. The AUC, sensitivity, and specificity of 3D DGS were 0.902 (0.818–0.985), 0.900 (0.714–1.000), and 0.890 (0.841–0.938), respectively, on the external testing set at quadrant level following normal clinical practice; and 0.885 (0.836–0.933), 0.912 (0.816–1.000), and 0.700 (0.660–0.741), respectively, on the external testing set at clock-hour level.

Conclusions: The 3D DGS is effective in detecting eyes with suspected PACG. It has the potential to be used widely in the primary eye care community for screening of subjects at high risk of developing PACG. *Ophthalmology 2022;129:45-53 © 2021 by the American Academy of Ophthalmology*

Supplemental material available at www.aaojournal.org.

Primary angle-closure glaucoma (PACG) is one of the major blinding eye conditions characterized by a narrow iridocorneal angle and glaucomatous optic neuropathy. It is projected that the number of people who have PACG worldwide will increase from 23 million to 32 million among the population aged more than 40 years between 2020 and 2040.[1] In China, PACG affects approximately 1.4% of citizens (19.6 million).[2-5] Compared with normal subjects, subjects with angle closure and peripheral anterior synechia (PAS) have a higher risk of progressing to PACG, because these factors may lead to elevated intraocular pressure (IOP).[6-8]

In clinical practice, the angle status of the eye, diagnosed using gonioscopy,[9,10] is crucial in determining the clinical progression and treatment management. Unfortunately, it is challenging for nonglaucoma specialists to master gonioscopy skills that are essential to determine the angle width (open or narrow) and the presence of PAS.[10] During static gonioscopy, the ophthalmologists will examine the extent and margin of the angle closure, whereas dynamic gonioscopy is used to detect the presence and extent of PAS along the iridocorneal angle. Based on the International Society of Geographical & Epidemiological Ophthalmology criteria or other

https://doi.org/10.1016/j.ophtha.2021.09.018
ISSN 0161-6420/21

international grading systems (e.g., Shaffer's grading system,[11] Scheie's grading system[12]), a narrow angle is defined as obscuration of the posterior trabecular meshwork for at least 180° under static gonioscopy.[13] Peripheral anterior synechia refers to the adhesions between the iris and the trabecular meshwork, which may lead to elevated IOP.[6,13] Peripheral anterior synechia also may be caused by various conditions, such as ocular inflammation, trauma, and acute angle-closure glaucoma. However, given that it is a contact examination, a number of patients experience discomfort and may not tolerate the examination well, resulting in difficulties in making an accurate assessment of the iridocorneal angle status and localization of PAS.

Anterior-segment OCT (AS OCT), combined with artificial intelligence, was previously reported in the evaluation of the iridocorneal angle,[14-17] but there are limitations, as follows. First, the evaluation was developed using few cross-sectional scans that did not cover the overall anterior chamber angle (ACA), which requires multiple cross-sectional scans of the same eye.[15,18-20] Thus, a 3-dimensional (3D) examination composed of a dense sampling of cross-sectional images may be more accurate to examine the angle status. Second, the ground truth used in previous studies was based on OCT scans but not clinical gonioscopic examination.[18,19] Third, static OCT performed under only 1 lighting condition is less useful to identify the existence and location of PAS.[21,22] Thus, the objective of this study was to develop and validate a deep-learning–based automated digital gonioscopy system (DGS) to detect narrow angle (Task I) on static examination and the presence of PAS (Task II) on dynamic examination under different lighting conditions (dark and bright) using swept-source OCT (SS-OCT). A flowchart of the study design is shown in Figure 1.

Methods

Data Preparation

The study was approved by the Ethics Review Committee of Zhongshan Ophthalmic Center (Guangzhou, China), the Singapore National Eye Centre (Singapore), and the Chulalongkorn University and King Chulalongkorn Memorial Hospital (Bangkok, Thailand) and was performed in accordance with the Declaration of Helsinki. Written informed consent was obtained from the participants.

The training and validation datasets were collected from the electronic medical database and research records at Zhongshan Ophthalmic Center from September 1, 2016, to September 1, 2019. The inclusion criteria in the study were as follows: (1) all participants must be aged ≥18 years; and (2) study subjects had a previous diagnosis of the ACA status (narrow or open, PAS or non-PAS) based on gonioscopy, SS-OCT scans, and medical history records. Exclusion criteria of the data included (1) poor compliance in receiving gonioscopy examination; (2) unclear AS-OCT scans due to blinking or out of focus; (3) recent use of miotics within 1 month; (4) secondary angle closure due to subluxation or dislocation, uveitis, or neovascular glaucoma; (5) history of ocular surgery or laser iridotomy; (6) patients who previously had an episode of primary angle closure (which was obtained on history by asking the patients).

For Task I, the external test dataset was obtained from the Singapore National Eye Centre, Singapore, from June 2008 to November 2019. For Task II, the external test dataset was obtained from the King Chulalongkorn Memorial Hospital, Bangkok, Thailand, from October 2019 to April 2020. All of the AS-OCT scans of a single patient were included in the training, validation, or test sets to ensure these datasets were unique at the patient level.

There were 7838 volume scans in Task I, which is divided into a training set of 4515 scans (3012 open and 1503 narrow), a validation set of 1101 scans (706 open and 395 narrow), and a test set of 2222 scans (1705 open and 517 close). There were 856 volume scans in Task II. Each volume scan was further divided into 12 clock-hour scans because the label of PAS was made on a clock-hour level. The data in Task II were divided into a training set of 4536 clock-hour scans (480 PAS and 4056 non-PAS), a validation set of 4512 clock-hour scans (576 PAS and 3936 non-PAS), and a test set of clock-hour 1224 scans (240 PAS and 984 non-PAS).

Ground Truth Labeling

On the basis of the gonioscopy results obtained with a Sussman 4-mirror gonioscope lens, narrow angles were defined as non-visibility of the posterior pigmented trabecular meshwork for more than 180° without indentation in the primary position examined in a dark room (0.4 lux).[13] Peripheral anterior synechia was defined as the adhesion of the iris to the trabecular meshwork wider than half a clock-hour. The existence and extent of PAS were determined using indentation gonioscopy in a dark room (0.4 lux) by glaucoma experts. Gonioscopy was performed on each eye twice by 2 independent observers from each center (Zhongshan Ophthalmic Center: F. Li, F. Lin, X.Z.; Singapore National Eye Centre: B.M., M.N., T.A.; King Chulalongkorn Memorial Hospital: S.C., K.R., A.M., V.T., P.R.). Gonioscopy was first performed by 1 grader and then validated by a senior glaucoma expert. The 2 observers would discuss to reach a consensus should there be a discordant finding; otherwise, the case would be excluded.

Anterior-Segment OCT Imaging

For each eye included, OCT imaging was performed within the same day of gonioscopy examination. CASIA OCT (Tomey) was used to capture the morphology of the anterior segment. The OCT examinations were performed by experienced technicians blinded to the clinical information of the patients. The current study mainly focused on 2 tasks: narrow angle detection (Task I) and PAS detection (Task II). For Task I, 3D morphology of the anterior chamber was scanned with the "angle analysis" mode in a dark room with a light intensity of 0.4 lux. "Angle analysis" mode contains 128 radial B-scans centered at the central cornea. For the task of PAS detection, paired volume OCT scans under different light intensity were captured for each subject to simulate dynamic gonioscopy. The dark OCT scans are 3D volume scans of the anterior chamber obtained with the "angle analysis" mode in a dark room with a light intensity of 0.4 lux, whereas the light OCT scans are volume scans of the anterior chamber repeated with the "angle analysis" mode in a room with a light intensity of 104 lux. The criteria used for acceptable images include clear visualization of the iridocorneal angle and iris. Video 1 (available at www.aaojournal.org) shows the capturing of the anterior chamber volume scan in the dark room.

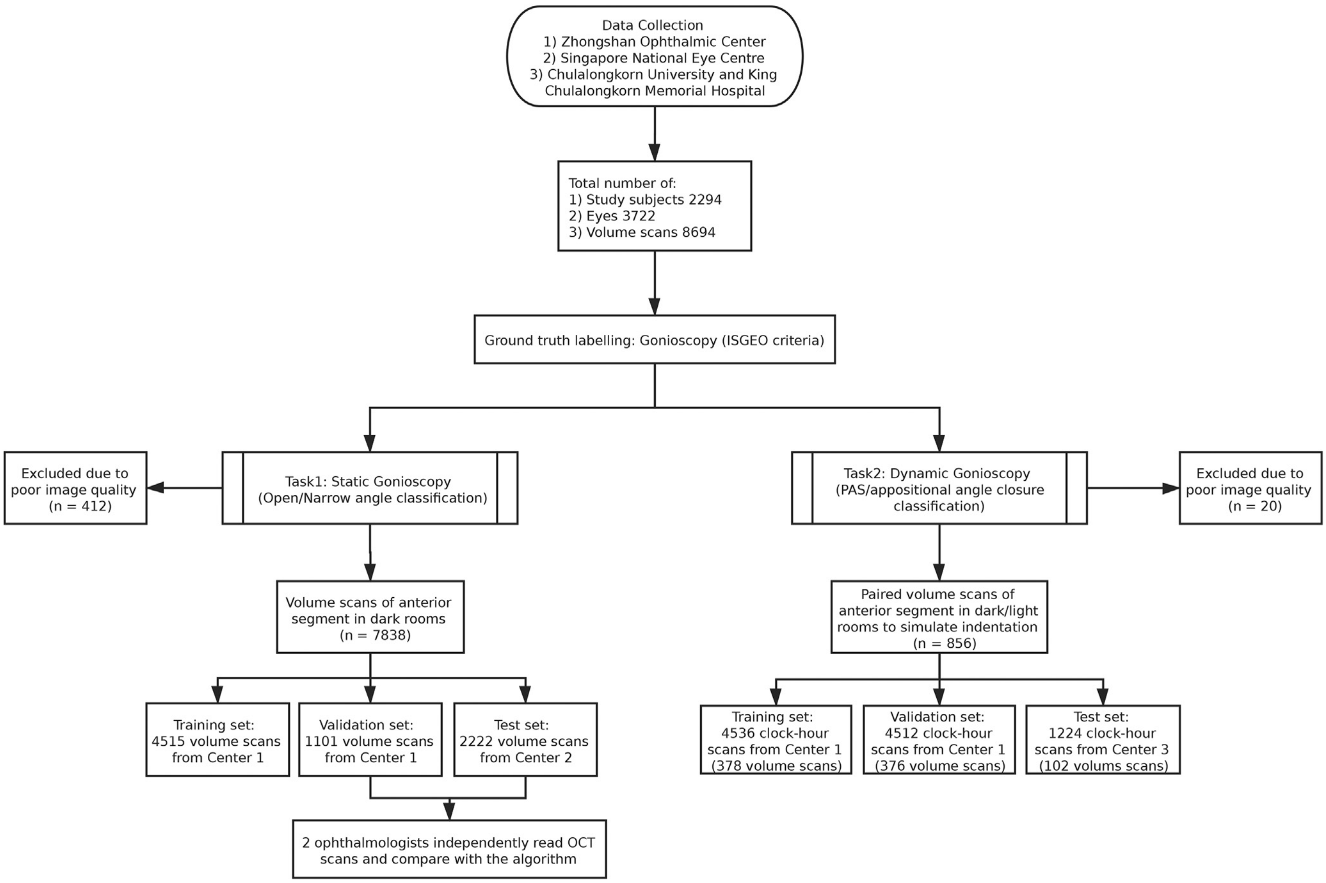

Figure 1. Flowchart of the current study. The study is composed of 2 tasks. In Task I, we developed the deep learning algorithm to simulate static gonioscopy for angle classification. In Task II, we developed the deep learning algorithm to simulate dynamic gonioscopy for peripheral synechia detection. ISGEO = International Society of Geographical & Epidemiological Ophthalmology; PAS = peripheral anterior synechiae.

Design and Development of the Digital Gonioscopy Systems

For Task I, we developed a 3D DGS to analyze the overall AS-OCT volume scan that analyzes the entire anterior chamber, using 3D-ResNet-34,[23,24] which contains 6 group learned layers. We cropped the original images in half. Then we flipped the half image of the right angle and concatenated all of them as input. For model training, we trained the model via SGD optimizer with a learning rate set to 0.1. We set the input image size to 512*128 and number of epochs to 200. The output was fed to the softmax layer, which produced a probability prediction over the 2 class labels (Fig S1, available at www.aaojournal.org).

For Task II, we used 2 sets of AS-OCT scans of the same eye, captured under dark (Dark DGS) and bright condition (Light DGS) to detect PAS, using 3D-ResNet-50 as the technical network.[25] The combination of Dark DGS and Light DGS is named "Paired DGS" in our study. Our previous study demonstrated that the DGS based on paired data had better performance than that based on single modal data (dark or light).[26] The synechia classification was analyzed using a dual-stream 3D deep learning system that models the dynamics of 2 different light conditions (Fig S2, available at www.aaojournal.org). Each clock-hour OCT scan consisted of 20 consecutive frames of ACA images. The images of 1 clock-hour were split in half first. Then the right part or left part of the images was selected depending on the specific hour. The half images were further cropped by a coarse to fine tool to extract the region of interest. Finally, 20 cropped images that represent a clock-hour were fed into our proposed neural networks. We trained the models for 200 epochs with a batch size of 8 and an input resolution of 244*244. After data preprocessing, the AS-OCT images captured in a dark room were fed into the dark stream, while its counterpart captured in a light room was fed into the light stream. The outputs of these 2 streams were then concatenated to produce the predictive score that indicated the possibility of synechial angle structure. To validate the superiority of the dual-stream fusion strategy, we also built single-stream counterparts of the deep-learning system, that is, Light DGS and Dark DGS, which only make use of AS-OCT volumes captured from one light condition. Although the OCT volume is input as a whole, it would be divided into 12 clock-hours after entering the neural network. Therefore, the probabilities of each clock-hour to have synechia could be generated independently (Fig S3, available at www.aaojournal.org).

The models were developed with Python (version 3.8.6) and PyTorch (version 1.6.0). To demonstrate the convergence of the algorithms regarding Tasks I and II, we show the curve of overall loss using TensorBoard (Fig S4, available at www.aaojournal.org). The key hyperparameters and average running time of each model are summarized in Table S1 (available at www.aaojournal.org). The gradient-weighted class activation mapping was applied to the DGS to generate heat maps on the key regions in the ACA suggestive of angle closure and PAS.[27]

Comparison of DGS versus General Ophthalmologists

For Task I, we also compared the diagnostic performance of DGS with 2 ophthalmologists (glaucoma specialists) who received ophthalmological training for more than 5 years. They did not participate in data collection or labeling and were blind to the ground truth. The 2 ophthalmologists were asked to classify the volume scans of 2465 eyes from 1435 subjects in the validation and external test sets into narrow versus open solely based on OCT scans without gonioscopy records. These 2 graders went through all the images in each volume scan for an eye and assigned 1 label (open/narrow) to it.

Statistics

The diagnostic performance of the DGS was calculated using the area under the curve (AUC) receiver operating characteristic, sensitivity, and specificity with a 95% confidence interval in the detection of narrow angle (Task I) and PAS (Task II). For Task I, we further compared the diagnostic performance of the 3D DGS with 2 general ophthalmologists. For Task II, we compared the diagnostic performance of the Paired DGS, Light DGS, and Dark DGS in PAS detection at both the clock-hour level and quadrant level (Fig S5, available at www.aaojournal.org). If there is no synechia in the 3 clock-hour scans within the same quadrant, the quadrant would be considered as nonsynechial; otherwise, the quadrant would be labeled as synechial. All statistical analyses were performed using R software (version 3.63). Data for continuous variables were presented as means and standard deviations. Wilcoxon rank-sum test was used for numerical data and chi-square test for categorical data to compare the difference between open-angle versus narrow-angle and PAS versus non-PAS groups. The characteristics of misclassified eyes were also analyzed. All the hypotheses tested were 2 sided, and we considered a P value of less than 0.05 to be statistically significant.

Results

Task I

Baseline Characteristics of the Data. A total of 1 003 264 cross-sectional scans from 7838 3D volume scans were obtained. The baseline characteristics of the study subjects in Task I are summarized in Table 1. There were significant differences in age and gender between the open-angle and narrow-angle groups. Details on the demographic characteristics in different datasets are shown in Table S2 (available at www.aaojournal.org).

Performance of the 3D DGS in Angle Width Classification in the Validation Sets. A total of 140 928 B-scans from 1101 volume scans captured by CASIA OCT were included in the validation set, which were collected from the Zhongshan Ophthalmic Center. The 3D DGS achieved an AUC of 0.994 (0.992−0.997), a sensitivity of 0.972 (0.956−0.988), and a specificity of 0.948 (0.931−0.964). The sensitivity of the 3D DGS was similar to that of Ophthalmologist 1 (0.975 [0.959−0.990], P = 0.99) and Ophthalmologist 2 (0.972 [0.956−0.988], P = 0.99) (Table 2 and Fig S6, available at www.aaojournal.org). The specificity of the 3D DGS was better than that of Ophthalmologist 1 (0.865 [0.840−0.901], P < 0.001) and Ophthalmologist 2 (0.885 [0.862−0.909], P < 0.001) (Table 2 and Fig S6, available at www.aaojournal.org).

Table 1. Demographic Information of Subjects in Task I and Task II

Task I Characteristics	Open-Angle Group	Narrow-Angle Group	P Value
Patients (eyes)	1364 (2437)	568 (857)	–
OCT scans	5423	2415	–
Sex (M/F)	629/733	172/388	<0.001
Left/Right	1205/1232	434/423	0.547
Age (yrs), Mean (SD)	55.2 (13.7)	62.6 (8.5)	<0.001
Ethnicity			
Chinese (%)	1238 (90.8)	536 (94.4)	–
Malaysian (%)	28 (2.1)	10 (1.8)	–
Indians (%)	64 (4.7)	18 (3.1)	–
Others (%)	34 (2.5)	4 (0.7)	–
Task II Characteristics	**PAS Group**	**Non-PAS Group**	**P Value**
Patients (eyes)	50 (54)	312 (374)	–
No. of OCT scans (clock hours)	1296	8976	–
No. of PAS units (clock hours)	716	0	–
Sex (M/F)	21/29	150/164	0.447
Left/Right	44/10	192/182	<0.001
Age (yrs), Mean (SD)	59.3 (9.5)	51.9 (15.2)	<0.001
Ethnicity			
Chinese (%)	40 (80)	271 (86.9)	–
Thai (%)	10 (20)	41 (13.1)	–

– = not available; F = female; M = male; PAS = peripheral anterior synechia; SD = standard deviation

Performance of the 3D DGS in Angle Width Classification in the External Test Set. A total of 284 416 B-scans from 2222 volume scans captured with CASIA OCT were included in the external test set, which were acquired from the Singapore National Eye Centre. The 3D DGS achieved an AUC of 0.943 (0.933−0.953), a sensitivity of 0.867 (0.838−0.895), and a specificity of 0.878 (0.859−0.896). The sensitivity of the 3D DGS was close to, although not as good as, that of Ophthalmologist 1 (0.892 [0.889−0.936], P = 0.03) and Ophthalmologist 2 (0.905 [0.880−0.930], P = 0.04). The specificity of the 3D DGS was similar to that of Ophthalmologist 1 (0.882 [0.864−0.894], P = 0.73) (Table 2 and Fig 2) and better than that of Ophthalmologist 2 (0.841 [0.820−0.861], P = 0.005) (Table 2 and Fig 2).

Figure S7 and Video 2 (available at www.aaojournal.org) display the heatmaps of the typical sample eyes with (left) and without (right) angle closure detected by the 3D DGS. The heatmaps indicated that the 3D DGS made a diagnosis based on the structures close to the ACA.

Characteristics of Misclassifications by the DGS. The characteristics of the misclassifications in the validation set by the 3D DGS are summarized in Table S3 (available at www.aaojournal.org). The reasons for 11 false-negative results mainly include shadow interference (3, 27.3%) and plateau iris (8, 72.7%). The 24 false-positive results are primarily due to shadow interference (22, 91.7%). Representative samples of misclassified OCT scans are shown in Figure S8 (available at www.aaojournal.org).

Table 2. Performance of the DGS Compared with the Ophthalmologists on the Validation and External Test Sets of Task I

	AUC (95% CI)	Sensitivity (95% CI)	P_1 Value*	Specificity (95% CI)	P_2 Value†
Validation Set (Zhongshan Ophthalmic Center)					
3D DGS	0.994 (0.992–0.997)	0.972 (0.956–0.988)		0.948 (0.931–0.964)	
Ophthalmologist 1		0.975 (0.959–0.990)	0.99	0.865 (0.840–0.901)	<0.001
Ophthalmologist 2		0.972 (0.956–0.988)	0.99	0.885 (0.862–0.909)	<0.001
External Test Set (Singapore National Eye Centre)					
3D DGS	0.943 (0.933–0.953)	0.867 (0.838–0.895)		0.878 (0.859–0.896)	
Ophthalmologist 1		0.892 (0.889–0.936)	0.03	0.882 (0.864–0.894)	0.73
Ophthalmologist 2		0.905 (0.880–0.930)	0.04	0.841 (0.820–0.861)	0.005

AUC = area under the curve; CI = confidence interval; DGS = deep-learning–based automated digital gonioscopy system; 3D = 3-dimensional.
*Comparison of sensitivities between ophthalmologists and 3D model using McNemar test.
†Comparison of specificities between ophthalmologists and 3D model using McNemar test.

Task II

Baseline Characteristics of the Data. We included 109 568 cross-sectional scans of 856 3D volume scans, which were further separated into 10 272 clock-hours of OCT scans in this task. The baseline characteristics of the study subjects in Task II are summarized in Table 1. There was a significant difference in age between the PAS and non-PAS groups. Details on the demographic characteristics in different datasets are shown in Table S4 (available at www.aaojournal.org).

Performance of the DGSs in PAS Detection in the Validation Set. A total of 4512 clock-hours of OCT scans captured with CASIA OCT were included in the validation set, which were collected from the Zhongshan Ophthalmic Center. The performance of the DGS in the detection of PAS was first tested at the level of clock-hour. The Paired DGS achieved the best diagnostic performance with an AUC of 0.941 (0.921–0.957), a sensitivity of 0.873 (0.820–0.925), and a specificity of 0.886 (0.873–0.900) (Table 3 and Fig S9A, available at www.aaojournal.org). Similar results were achieved when evaluating the diagnostic performance of the DGSs on the quadrant level.

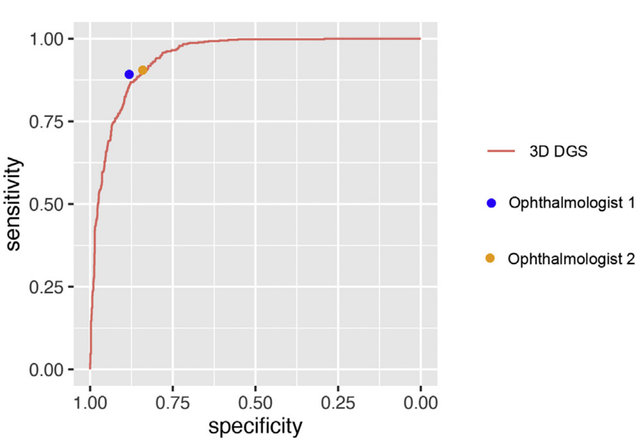

Figure 2. Comparison of diagnostic performance of the 3-dimensional (3D) deep-learning–based automated digital gonioscopy system (DGS) in angle classification with ophthalmologists in the external test set. The figure shows receiver operating curve of angle classification by the 3D DGS with an area under the curve (AUC) of 0.943 (0.933–0.953).

The Paired DGS had an AUC of 0.959 (0.943–0.975), a sensitivity of 0.909 (0.840–0.978), and a specificity of 0.914 (0.893–0.935) (Table 3 and Fig S9B, available at www.aaojournal.org).

Performance of the DGS in PAS Detection in External Test Set. A total of 1224 clock-hours of OCT scans captured with CASIA OCT were included in the external test set, which were acquired from the Chulalongkorn University and King Chulalongkorn Memorial Hospital, Thailand. At the clock-hour level, the Paired DGS outperformed the other DGSs in PAS detection with an AUC of 0.885 (0.836–0.933), a sensitivity of 0.912 (0.816–1.000), and a specificity of 0.700 (0.660–0.741) (Table 3 and Fig 3A). Similar results were achieved when evaluating the DGSs at the quadrant level. The Paired DGS had an AUC of 0.902 (0.818–0.985), a sensitivity of 0.900 (0.714–1.000), and a specificity of 0.890 (0.841–0.938) (Table 3 and Fig 3B).

Figure S10 and Video 3 (available at www.aaojournal.org) display the heatmaps of the typical sample eyes with and without PAS detected by the Paired DGS. The heatmaps indicated that the Paired DGS detected PAS by comparing the morphological change of the iris adjacent to the iridocorneal angle, mainly the iris root and the middle part of the iris.

Characteristics of Misclassifications by the DGS. The 259 misclassified samples by the Paired DGS in the validation set are summarized in Table S5 (available at www.aaojournal.org). The features of 19 false-negative results were mainly due to point synechia (15, 78.9%), whereas the 240 false-positive results were primarily due to iridauxesis (149, 62.0%) and plateau iris (91, 38.0%). Representative samples of misclassified OCT scans are shown in Figure S11 (available at www.aaojournal.org).

Discussion

The current research involves the largest AS-OCT datasets of more than 1 million labeled cross-sectional scans with clinical diagnosis based on gonioscopy. We designed a 3D DGS, simulating both static and dynamic gonioscopy to detect narrow-angle subjects and PAS. In Task I, we demonstrated that the 3D DGS achieved diagnostic performance close to that of the ophthalmologists in angle width

Table 3. Performance of DGS for PAS Detection in the Validation and External Test Sets of Task II

Validation Set (Zhongshan Ophthalmic Center)				
Clock-Hour Level	*AUC (95% CI)*	*Sensitivity (95% CI)*	*Specificity (95% CI)*	*P Value**
Light DGS†	0.933 (0.913–0.953)	0.904 (0.858–0.950)	0.898 (0.885–0.911)	0.294
Dark DGS†	0.927 (0.903–0.950)	0.834 (0.776–0.893)	0.920 (0.908–0.932)	0.100
Paired DGS†	0.941 (0.921–0.957)	0.873 (0.820–0.925)	0.886 (0.873–0.900)	–
Quarter level	**AUC (95% CI)**	**Sensitivity (95% CI)**	**Specificity (95% CI)**	**P Value***
Light DGS	0.947 (0.927–0.967)	0.924 (0.860–0.988)	0.882 (0.858–0.906)	0.090
Dark DGS	0.939 (0.908–0.969)	0.924 (0.860–0.988)	0.863 (0.837–0.889)	0.092
Paired DGS	0.959 (0.943–0.975)	0.909 (0.840–0.978)	0.914 (0.893–0.935)	–
External Test Set (Chulalongkorn University and King Chulalongkorn Memorial Hospital)				
Clock-Hour Level	*AUC (95% CI)*	*Sensitivity (95% CI)*	*Specificity (95% CI)*	*P Value**
Light DGS	0.754 (0.678–0.830)	0.882 (0.774–0.991)	0.555 (0.511–0.598)	0.007
Dark DGS	0.549 (0.458–0.639)	0.824 (0.695–0.952)	0.310 (0.269–0.350)	<0.001
Paired DGS	0.885 (0.836–0.933)	0.912 (0.816–1.000)	0.700 (0.660–0.741)	–
Quarter Level	**AUC (95% CI)**	**Sensitivity (95% CI)**	**Specificity (95% CI)**	**P Value***
Light DGS	0.611 (0.423–0.799)	0.800 (0.552–1.000)	0.485 (0.408–0.561)	0.008
Dark DGS	0.412 (0.227–0.596)	0.600 (0.296–0.904)	0.485 (0.408–0.561)	<0.001
Paired DGS	0.902 (0.818–0.985)	0.900 (0.714–1.000)	0.890 (0.841–0.938)	–

– = not available; AUC = area under the curve; CI = confidence interval; DGS = digital gonioscopy system; PAS = peripheral anterior synechia.
*Comparison of AUC of Light DGS and Dark DGS with Paired DGS using Z test.
†The synechia classification was analyzed using a dual-stream 3D deep learning system, which is named "Paired DGS." After data preprocessing, the AS OCT scans captured in a darkroom are fed into the dark stream, while its counterpart captured in a lightroom is fed into the light stream. The outputs of these 2 streams are then concatenated as the Paired DGS. To validate the superiority of the dual-stream fusion strategy, we also built single-stream counterparts of the deep-learning system, that is, Light DGS and Dark DGS, which only use AS OCT volumes captured from 1 light condition (light or dark).

classification based on OCT scans. In Task II, the Paired DGS was designed to simulate dynamic gonioscopy and detect PAS based on paired OCT scans of different light intensity, which achieved an AUC of 0.902 at quadrant level. To our knowledge, this is the first deep learning research simultaneously covering both static and dynamic gonioscopy, and the detection of PAS based on OCT scans was explored in a previous study by our team.[26]

Gonioscopy has been the clinical standard for PACG diagnosis; however, it is a contact examination with an extended learning curve. Angle width classification is determined by static gonioscopy, whereas PAS detection relies on dynamic gonioscopy. In recent years, AS-OCT has been used more frequently in PACG diagnosis because it is rapid and less dependent on patient cooperation and examiner skills. Previous studies focused on

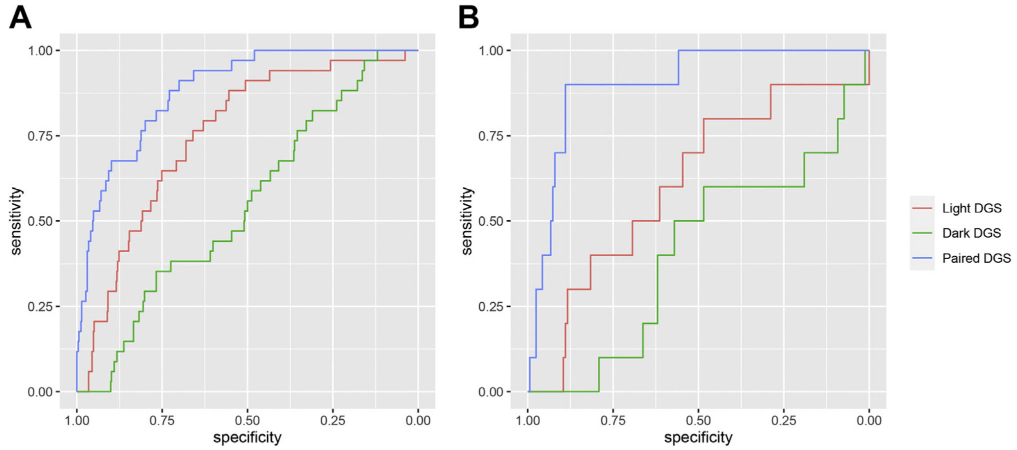

Figure 3. Comparison of diagnostic performance of the deep-learning–based automated digital gonioscopy system (DGS) in peripheral anterior synechia (PAS) detection in the external test set. The Paired DGS using paired light and dark data achieved the best diagnostic performance with an area under the curve (AUC) of 0.885 (0.836–0.933) at clock-hour level **(A)** and an AUC of 0.902 (0.818–0.985) at quadrant level **(B)**.

developing machine learning algorithms for angle width classification based on OCT scans, similar to static gonioscopy. By using 8270 images (7375 open-angle and 895 narrow-angle images), Fu et al[19] reported that the deep learning model yielded an AUC of 0.96 in angle classification, which is better than angle-closure detection using quantitative features. In another study by Fu et al,[14] the researchers further tested different algorithms in OCT images from other devices, including Visante, Cirrus HD, and CASIA. The algorithm with the best performance achieved an AUC of 0.962. Xu et al[16] developed an automated algorithm to classify open and narrow angles with 4036 (1943 open, 2093 narrow) SS-OCT images. The algorithm based on ResNet-18 architecture achieved an AUC of 0.933, which could be used to improve PACG screening in high-risk populations.

Compared with previous research on angle width classification, our study has several strengths. First, the ground truth of our study was based on gonioscopy records and coherent with clinical practice, whereas the ground truth of previous studies was based on AS-OCT scans but not gonioscopy.[18,19] Second, our definition of narrow angle strictly follows the International Society of Geographical & Epidemiological Ophthalmology criteria[13] and depends on the evaluation of the whole iridocorneal angle but not a single cross-section. We have developed the 3D DGS to classify the angles based on the general morphology of the volume scans. The 3D DGS is a new design, with all of the volume scans as the input and a comprehensive evaluation of all the related structures in the anterior segment. The 3D DGS achieved an AUC of 0.994 and 0.943 in the validation and external test sets, respectively. In general, the level of gonioscopy skills among comprehensive ophthalmologists is highly variable, leading to differences in examination quality and ultimate diagnosis of angle closure. In comparison with the 2 ophthalmologists from Zhongshan Ophthalmic Center who had more than 5 years of training in glaucoma, the algorithm achieved performance similar to that of the specialists in angle width classification. Therefore, the algorithm would be useful in assisting non-glaucoma specialists in screening angle-closure subjects.

Another innovation of the current study is the design of the DGS to detect PAS, which has been explored in our pilot study.[26] Determination of the existence and extent of PAS is also crucial in PACG diagnosis and treatment strategy. Indentation gonioscopy involves pressure on the peripheral anterior chamber to differentiate appositional angle closure from PAS. Because this is a dynamic process, we cannot simulate it with a single OCT scan, and it is difficult to determine the location of PAS based on OCT scans. When the environment changes from dark to light, the morphology of the iris will change because of the contraction of the sphincter pupillae. Therefore, paired OCT scans under different light intensity were performed to simulate the dynamic changes under indentation gonioscopy, as indicated in a previous study by Leung et al.[28] In our previous research, we developed and tested the performance of multiple algorithms based on paired dark-light data to detect PAS,[26] which achieved a highest AUC of 0.844 in a smaller dataset of 100 eyes. The study also showed that the algorithms based on paired data had better performance than those based on single modal data (dark or light).[26] With these paired scans as training data, the Paired DGS achieved an AUC of 0.885 at the clock-hour level and 0.902 at the quadrant level on the external test set with 1228 samples. We also noticed a 0.05 reduction (0.885 vs. 0.941, 0.902 vs. 0.959) of AUC in the test set compared with the validation set, which is likely due to different ethnic backgrounds (Chinese vs. Thai), sample size, and data distribution (older age, more eyes with synechia in the test set) in these datasets. More data with various ethnic groups, age, and gender could further improve the diagnostic performance of the Paired DGS in PAS detection. The diagnostic performance of the Paired DGS was superior to that of the Light DGS in the external test data, although there was no significant difference between the AUCs of the Paired DGS and Light DGS in the validation set. In general, these results indicate that a combination of light and dark OCT scans is an excellent simulation of dynamic gonioscopy, and its diagnostic performance remained stable in different datasets.

In Task I, shadow interference in OCT scans is a common reason for errors. Another reason for false-negative errors is plateau iris. Plateau iris refers to an iris with a flat central surface and angulated sharp drop-off of the peripheral portion next to the angle wall,[29] which may confuse the algorithm as an open angle.

In Task II, according to the heatmaps, the Paired DGS detected the PAS by identifying if there was a morphological change of the iris in the paired light and dark OCT scans. Point synechia is the main reason of false-negative errors. Because point synechia only exists in several frames of the OCT scans, mostly less than 3 frames, the Paired DGS cannot identify it from the adjacent OCT scans. Iridauxesis and plateau iris are the main reasons for false-positive results. In eyes with iridauxesis and plateau iris, the morphological change of the iris between light and dark conditions mainly happens in the middle part of the iris, similar to the condition of synechia. Thus, the algorithms misclassified these cases as synechia cases.

Study Limitations

The limitations of this study should be considered. First, our study was based on clinical data of an Asian population (Chinese, Indians, and Malaysians), and the performance of the algorithm has not been verified in other population ethnicities. Second, the DGSs were mainly based on CASIA SS-OCT. It is also necessary to test its performance in images from other devices that could capture 3D volume scans of the anterior segment. Third, the Paired DGS is designed to differentiate PAS from appositional angle closure automatically. Its performance to detect point synechia is relatively poor. Fourth, the algorithm was designed to classify the angle into narrow and open. It could not further classify the narrow angles into different grades.

In conclusion, we have developed a reliable DGS that not only could differentiate PACG subjects from normal subjects but also could determine the location and range of PAS in the iridocorneal angle. We believe the system would be promising as an excellent adjunct and potential replacement of gonioscopy in specific clinical settings.

Footnotes and Disclosures

Originally received: June 7, 2021.
Final revision: September 18, 2021.
Accepted: September 28, 2021.
Available online: October 5, 2021. Manuscript no. D-21-01152.

[1] State Key Laboratory of Ophthalmology, Zhongshan Ophthalmic Center, Sun Yat-sen University, Guangzhou, People's Republic of China.

[2] School of Software Engineering, South China University of Technology, Guangzhou, People's Republic of China.

[3] Intelligent Healthcare Unit, Baidu, People's Republic of China.

[4] Singapore Eye Research Institute, Singapore.

[5] Singapore National Eye Centre and Duke-NUS Medical School, Singapore.

[6] Glaucoma Research Unit, Faculty of Medicine, Chulalongkorn University and King Chulalongkorn Memorial Hospital, Thai Red Cross, Bangkok, Thailand.

[7] Yong Loo Lin School of Medicine, National University of Singapore, Singapore.

*Fei Li, Yifan Yang, and Xu Sun contributed equally to this work.

Disclosure(s):

All authors have completed and submitted the ICMJE disclosures form.

The author(s) have no proprietary or commercial interest in any materials discussed in this article.

Supported by the High-level Hospital Construction Project, Zhongshan Ophthalmic Center, Sun Yat-sen University (303020104), and the Science and Technology Program of Guangzhou, China (2021).

The study protocol can be accessed at clinicaltrials.gov (Registration ID: NCT04242108). The datasets used in this study originated from different principal investigators in China, Singapore, and Thailand.

Tin Aung and Daniel S.W. Ting are editorial board members of this journal, were recused from the peer-review process of this article and had no access to information regarding its peer-review.

HUMAN SUBJECTS: Human subjects were included in this study. The study was approved by the Ethics Review Committee of Zhongshan Ophthalmic Center (ZOC, Guangzhou, China), Singapore National Eye Centre (SERI, Singapore), and the Chulalongkorn University and King Chulalongkorn Memorial Hospital (KCMH, Bangkok, Thailand), and was performed in accordance with the Declaration of Helsinki. Written informed consents were obtained from the participants.

No animal subjects were used in this study.

Author Contributions:

Conception and design: Li, Yang, Tan, Aung, Xu, Zhang

Data collection: Li, Yang, Sun, Qiu, Zhang, Tun, Mani, Nongpiur, Chansangpetch, Ratanawongphaibul, Manassakorn, Tantisevi, Rojanapongpun, Lin, Cheng, Zhou, Liu, Chen, Xiong, Tan, Xu, Zhang

Analysis and interpretation: Li, Yang, Sun, Qiu, Aung, Xu, Ting, Zhang

Obtained funding: Zhang

Overall responsibility: Li, Yang, Sun, Aung, Xu, Ting, Zhang

Abbreviations and Acronyms:
ACA = anterior chamber angle; **AS OCT** = anterior-segment OCT; **AUC** = area under the curve; **DGS** = deep-learning−based automated digital gonioscopy system; **IOP** = intraocular pressure; **PACG** = primary angle-closure glaucoma; **PAS** = peripheral anterior synechia; **SS-OCT** = swept-source OCT; **3D** = 3-dimensional.

Keywords:
Angle closure, Anterior segment OCT, Deep learning, Glaucoma.

Correspondence:
Xiulan Zhang, MD, PhD, State Key Laboratory of Ophthalmology, Zhongshan Ophthalmic Center, Sun Yat-sen University, Guangzhou, People's Republic of China. E-mail: zhangxl2@mail.sysu.edu.cn; Yanwu Xu, PhD, Intelligent Healthcare Unit, Baidu, People's Republic of China. E-mail: ywxu@ieee.org; Mingkui Tan, PhD, School of Software Engineering, South China University of Technology, Guangzhou, People's Republic of China. E-mail: mingkuitan@scut.edu.cn; Tin Aung, MD, PhD, Singapore National Eye Centre and Duke-NUS Medical School, Singapore. E-mail: aung.tin@singhealth.com.sg.

References

1. Tham Y-C, Li X, Wong TY, et al. Global prevalence of glaucoma and projections of glaucoma burden through 2040: a systematic review and meta-analysis. *Ophthalmology*. 2014;121:2081−2090.
2. Liang Y, Friedman DS, Zhou Q, et al. Prevalence and characteristics of primary angle-closure diseases in a rural adult Chinese population: The Handan Eye Study. *Investig Ophthalmol Vis Sci*. 2011;52:8672−8679.
3. Qu W, Li Y, Song W, et al. Prevalence and risk factors for angle-closure disease in a rural Northeast China population: a population-based survey in Bin County, Harbin. *Acta Ophthalmologica*. 2011;89:e515−e520.
4. Wang YX, Xu L, Yang H, Jonas JB. Prevalence of glaucoma in North China: The Beijing Eye Study. *Am J Ophthalmol*. 2010;150:917−924.
5. Cheng J-W, Cheng S-W, Ma X-Y, et al. The prevalence of primary glaucoma in mainland China: a systematic review and meta-analysis. *J Glaucoma*. 2013;22:301−306.
6. Foster P, Aung T, Nolan W, et al. Defining "occludable" angles in population surveys: drainage angle width, peripheral anterior synechiae, and glaucomatous optic neuropathy in east Asian people. *Br J Ophthalmol*. 2004;88:486−490.
7. Amerasinghe N, Aung T. Angle-closure: risk factors, diagnosis and treatment. In: Nucci C, Cerulli L, Osborne NN, Bagetta G, eds. *Progress in Brain Research*. NY: Elsevier; 2008:173. v.
8. He M, Foster PJ, Ge J, et al. Gonioscopy in adult Chinese: The Liwan Eye Study. *Investig Ophthalmol Vis Sci*. 2006;47:4772−4779.
9. Troncoso MU. Gonioscopy and its clinical applications. *Am J Ophthalmol*. 1925;8:432b−449.

10. Forbes M. Gonioscopy with corneal indentation: a method for distinguishing between appositional closure and synechial closure. *Arch Ophthalmol*. 1966;76:488−492.
11. Shaffer RN. Stereoscopic manual of gonioscopy. *Acad Med*. 1963;38:529.
12. Scheie HG. Width and pigmentation of the angle of the anterior chamber: a system of grading by gonioscopy. *AMA Arch Ophthalmol*. 1957;58:510−512.
13. Foster PJ, Buhrmann R, Quigley HA, Johnson GJ. The definition and classification of glaucoma in prevalence surveys. *Br J Ophthalmol*. 2002;86:238−242.
14. Fu H, Xu Y, Lin S, et al. Angle-closure detection in anterior segment OCT based on multilevel deep network. *IEEE Trans Cybern*. 2019:1−9.
15. Fu H, Xu Y, Lin S, et al. Segmentation and quantification for angle-closure glaucoma assessment in anterior segment OCT. *IEEE Trans Med Imaging*. 2017;36:1930−1938.
16. Xu BY, Chiang M, Chaudhary S, et al. Deep learning classifiers for automated detection of gonioscopic angle closure based on anterior segment OCT images. *Am J Ophthalmol*. 2019;208:273−280.
17. Shan J, DeBoer C, Xu BY. Anterior segment optical coherence tomography: applications for clinical care and scientific research. *Asia Pac J Ophthalmol (Phila)*. 2019. https://doi.org/10.22608/APO.201910.
18. Fu H, Xu Y, Lin S, et al. Angle-closure detection in anterior segment OCT based on multilevel deep network. *IEEE Trans Cybern*. 2020;50:3358−3366.
19. Fu H, Baskaran M, Xu Y, et al. A deep learning system for automated angle-closure detection in anterior segment optical coherence tomography images. *Am J Ophthalmol*. 2019;203:37−45.
20. Porporato N, Tun TA, Baskaran M, et al. Towards 'automated gonioscopy': a deep learning algorithm for 360° angle assessment by swept-source optical coherence tomography. *Br J Ophthalmol*. 2021. bjophthalmol-2020-318275.
21. Masoodi H, Jafarzadehpur E, Esmaeili A, et al. Evaluation of anterior chamber angle under dark and light conditions in angle closure glaucoma: an anterior segment OCT study. *Cont Lens Anterior Eye*. 2014;37:300−304.
22. Hirose F, Hata M, Ito S-I, et al. Light−dark changes in iris thickness and anterior chamber angle width in eyes with occludable angles. *Graefes Arch Clin Exp Ophthalmol*. 2013;251:2395−2402.
23. Hara K, Kataoka H, Satoh Y. Can spatiotemporal 3D CNNs retrace the history of 2D CNNs and ImageNet? Proceedings of the IEEE Conference on Computer Vision and Pattern Recognition. 2018.
24. Hara K, Kataoka H, Satoh Y. Learning spatio-temporal features with 3D residual networks for action recognition. Proceedings of the IEEE International Conference on Computer Vision Workshops. 2017.
25. He K, Zhang X, Ren S, Sun J. Deep residual learning for image recognition. 2016 IEEE Conference on Computer Vision and Pattern Recognition (CVPR). 2016.
26. Hao H, Zhao Y, Yan Q, et al. Angle-closure assessment in anterior segment OCT images via deep learning. *Med Image Anal*. 2021;69:101956.
27. Selvaraju RR, Cogswell M, Das A, et al. Grad-cam: visual explanations from deep networks via gradient-based localization. Proceedings of the IEEE International Conference on Computer Vision. 2017.
28. Lai I, Mak H, Lai G, et al. Anterior chamber angle imaging with swept-source optical coherence tomography: measuring peripheral anterior synechia in glaucoma. *Ophthalmology*. 2013;120:1144−1149.
29. Ritch R. Plateau iris is caused by abnormally positioned ciliary processes. *J Glaucoma*. 1992;1:23−26.